การวิเคราะห์บาวดารีเอลิเมนต์ของชิ้นส่วนไพอิโซอิเล็กทริกสองวัสดุ

ธีรพงศ์ เสนจันทร์ฒิไชย [1] **และ จารุวัจน์ วิรัชพงศานนท์** [2]

จุฬาลงกรณ์มหาวิทยาลัย วังใหม่ ปทุมวัน กรุงเทพฯ 10330

รับเมื่อ 4 ธันวาคม 2549 ตอบรับเมื่อ 8 พฤษภาคม 2550

บทคัดย่อ

บทความฉบับนี้นำเสนอการวิเคราะห์แผ่นระนาบชิ้นส่วนไพอิโซอิเล็กทริกสองวัสดุภายใต้แรงกระทำทางกลหรือโหลดทางไฟฟ้าด้วยระเบียบวิธีบาวดารีเอลิเมนต์โดยอาศัยสมการเชิงปริพันธ์ขอบเขตทางตรง และใช้ฟังก์ชันของกรีนจากการให้น้ำหนักบรรทุกและประจุไฟฟ้าหนึ่งหน่วย การพัฒนาโปรแกรมบาวดารีเอลิเมนต์ทำโดยใช้การประยุกต์แบบจำลองบริเวณย่อยและการประกอบระบบสมการพีชคณิตหลายบริเวณ การลู่เข้าและความมีเสถียรภาพของผลลัพธ์ ตลอดจนความถูกต้องของคำตอบได้ถูกตรวจสอบกับคำตอบเชิงวิเคราะห์จากงานวิจัยในอดีต ได้นำเสนอผลวิเคราะห์แผ่นระนาบชิ้นส่วนไพอิโซอิเล็กทริกสองวัสดุที่มีรูกลวงชนิดวงรีภายใต้แรงกระทำทางกลหรือโหลดทางไฟฟ้า เพื่อแสดงถึงอิทธิพลของลักษณะความบกพร่องต่อหน่วยแรงการกระจัดทางไฟฟ้าและสนามไฟฟ้ารอบรูกลวงและตามแนวรอยต่อประสานของชิ้นส่วนไพอิโซอิเล็กทริกสองวัสดุ

คำสำคัญ : ระเบียบวิธีบาวดารีเอลิเมนต์ / ความบกพร่อง / รอยต่อประสาน / วัสดุไพอิโซอิเล็กทริก

---

[1] *รองศาสตราจารย์ ภาควิชาวิศวกรรมโยธา*

[2] *อดีตนิสิตบัณฑิตศึกษา ภาควิชาวิศวกรรมโยธา*

Boundary Element Analysis of Piezoelectric Bi-Materials

Teerapong Senjuntichai [1] and Jaruwat Wiratchpongsanon [2]

Chulalongkorn University, Wangmai, Patumwan, Bangkok 10330

Received 4 December 2006 ; accepted 8 May 2007

Abstract

This paper presents boundary element analysis of two-dimensional piezoelectric bi-materials under mechanical or electrical loading. A direct formulation of the boundary integral equation is derived by employing closed form Green's functions for a two-dimensional piezoelectric solid subjected to concentrated line loads and a line electrical charge, and utilizing a sub-region model and a multi-region assembly. The convergence and numerical stability of the numerical solution scheme are established, and the accuracy is verified by comparing with existing analytical solutions. Selected numerical results for piezoelectric bi-materials with an elliptical hole due to remote mechanical or electrical loading are presented to portray the influence of geometry of defects on stresses, electric displacement and electric field around the hole and along the interface of piezoelectric bi-materials.

Key words : Boundary Element Method / Defects / Interface / Piezoelectric Materials

[1] *Associate Professor, Department of Civil Engineering.*

[2] *Former Graduate Student, Department of Civil Engineering.*

1. Introduction

Piezoelectric materials are widely used in the development of smart structures. These materials generate an electric charge in response to mechanical deformations and undergo deformations under an applied electric field. Relatively low tensile strength and fracture toughness are among the major concerns that limit the industrial applications of piezoelectric materials. Defects such as cavities, inclusions and cracks in these materials resulting from manufacturing processes could lead to undesirable performance.

Analytical solutions to boundary value problems involving piezoelectric solids with defects have been reported in the literature [1-4]. Only problems under ideal loading and geometries can be solved by using analytical methods. In recent years, the boundary element method (BEM) has emerged as a versatile computational tool for analysis of piezoelectric materials. This method requires only discretization of the boundary and its solutions in the vicinity of defects and material interface can be computed very accurately by using the boundary integral equations. Boundary element solutions for a piezoelectric solid with a hole were given by Lee [5], Ding et al. [6], Xu and Rajapakse [7] and Liu and Fan [8]. In addition, Pan [9], Davi and Milazzo [10] and Groh and Kuna [11] employed the boundary element method to determine stress intensity factors in a cracked piezoelectric medium.

This paper presents the application of a boundary element method for two-dimensional piezoelectric bi-materials with an elliptical cavity under electromechanical loading as shown in Fig. 1. The problem is considered as a piezoelectric domain consisting of two sub-regions with different material properties (Fig. 2). The boundary integral equation formulation employs closed form Green's functions, given by Rajapakse [12], corresponding to a piezoelectric solid subjected to concentrated line loads and a line electrical charge. The global equation system is assembled by considering the interface continuity conditions between the two domains. The convergence, numerical stability and accuracy of the boundary element solution are verified by comparing with analytical solutions given by Sosa [1]. Selected numerical results for stresses, electric displacements and electric fields around the hole and along the interface of piezoelectric bi-materials subjected to remote mechanical and electrical loads are presented.

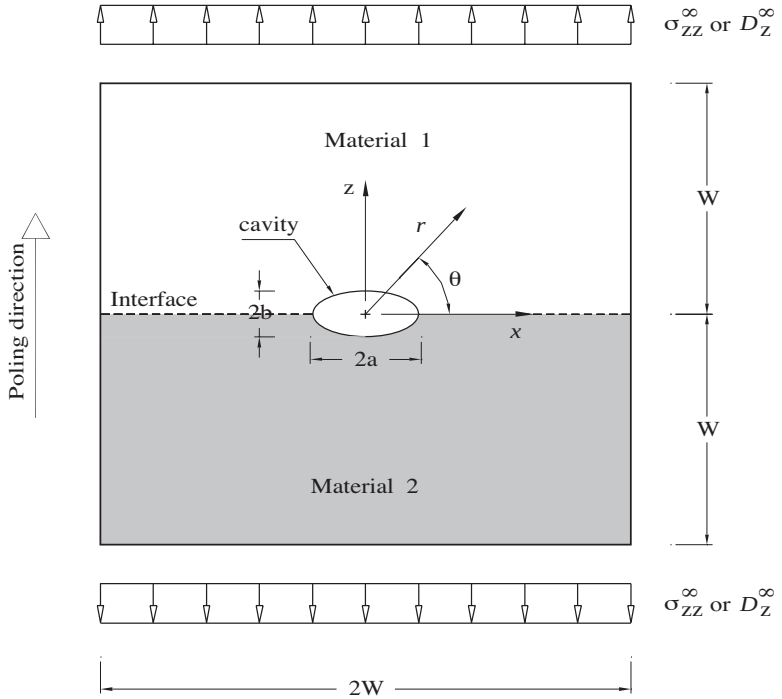

Fig. 1 Piezoelectric bi-materials with an elliptical cavity under electromechanical loading.

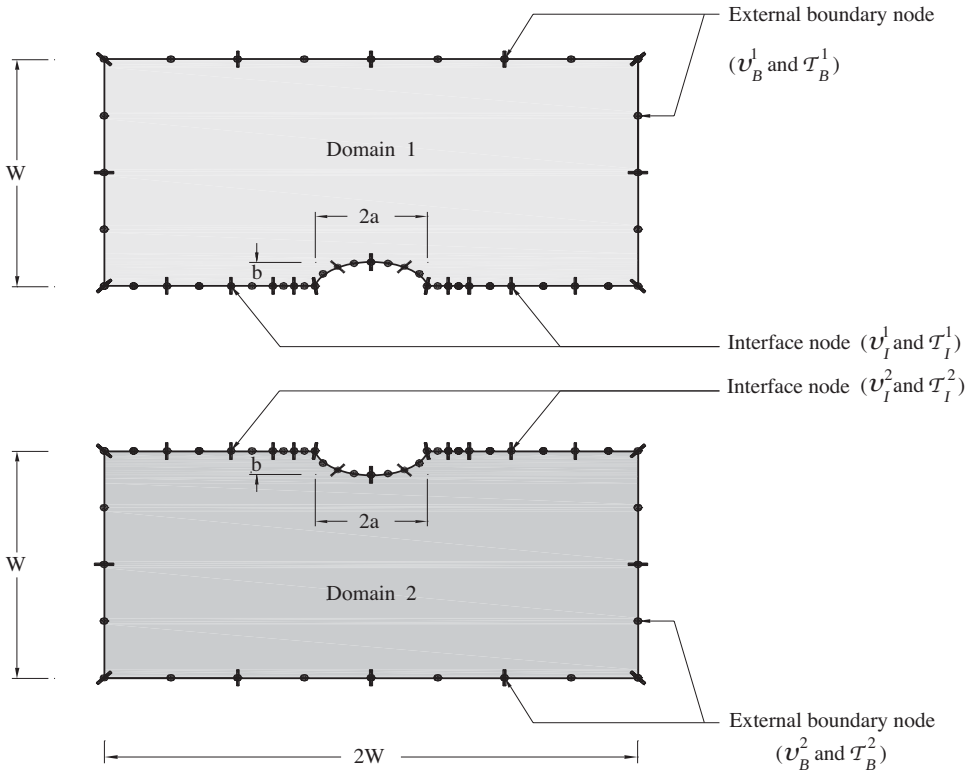

Fig. 2 Boundary element discretization.

2. Basic Equations

Consider a piezoelectric medium with a Cartesian coordinate system (*x, y, z*) defined such that the *z*-axis is the poling direction as shown in Fig.1. Constitutive relations for a piezoelectric material subjected to plane-strain deformations in the *x - z* plane, i.e. $\in_{xy} = \in_{yy} = \in_{yz} = E_y = 0$ can be expressed as follows:

$$\sigma_{xx} = c_{11} \in_{xx} + c_{13} \in_{zz} - e_{31} E_z \quad \textbf{(1)}$$

$$\sigma_{zz} = c_{13} \in_{xx} + c_{33} \in_{zz} - e_{33} E_z \quad \textbf{(2)}$$

$$\sigma_{xz} = 2c_{44} \in_{xz} - e_{15} E_x \quad \textbf{(3)}$$

$$D_x = 2e_{15} \in_{xz} + \varepsilon_{11} E_x \quad \textbf{(4)}$$

$$D_z = e_{31} \in_{xx} + e_{33} \in_{zz} + \varepsilon_{33} E_z \quad \textbf{(5)}$$

where σ_{ij}, $\in_{ij}$, D_i and E_i ($i, j = x, z$) are the components of stress, strain, electric displacement and electric field respectively; c_{11}, c_{13}, c_{33} and c_{44} are elastic constants under zero or constant electric field; e_{31}, e_{33} and e_{15} are piezoelectric coefficients; and ε_{11}, ε_{33} are dielectric constants under zero or constant strain. Table1 presents the electroelastic properties of PZT-4, PZT-5 and PZT-5H.

The constitutive equations for plane-stress response ($\sigma_{xy} = \sigma_{yy} = \sigma_{yz} = D_y = 0$) can be obtained from Eqs.(1) to (5) by replacing c_{11}, c_{13}, c_{33}, e_{31}, e_{33} and ε_{33} by $(c_{11} - c_{12}^2/c_{11})$, $(c_{13} - c_{12}c_{13}/c_{11})$, $(c_{33} - c_{13}^2/c_{11})$, $(e_{31} - c_{12}\, e_{31}/c_{11})$, $(e_{33} - c_{13}e_{31}/c_{11})$ and $(\varepsilon_{33} + e_{31}^2/c_{11})$ respectively.

The field equations for plane-stress/strain response of a piezoelectric material can be expressed by using the standard indicial notation as

$$\sigma_{ij,j} + F_i = 0; \quad D_{i,i} = \rho_e, \quad i, j = x, z \quad \textbf{(6)}$$

in which F_i and ρ_e denote the body force in the i-direction and a body electric charge respectively.

The strain-displacement and electric field-potential relations can be expressed as

$$\in_{ij} = \frac{1}{2}(u_{i,j} + u_{j,i}); \quad E_i = \phi_{,i}, \quad i, j = x, z \quad \textbf{(7)}$$

where u_i and ϕ denote the mechanical displacement in the i-direction and electric potential respectively.

Table 1 Material properties

	c_{11}^*	c_{12}^*	c_{13}^*	c_{33}^*	c_{44}^*	$e_{15}^\dagger$	$e_{31}^\dagger$	$e_{33}^\dagger$	$\varepsilon_{11}^\hbar$	$\varepsilon_{33}^\hbar$
PZT-4	13.9	7.78	7.43	11.3	2.56	13.44	-6.98	13.84	6.0	5.47
PZT-5	12.1	7.54	7.52	11.1	2.11	12.3	-5.4	15.8	8.170	7.346
PZT-5H	12.6	5.5	5.3	11.7	3.53	17.0	-6.5	23.3	15.1	13.0

$^*\times 10^{10}$ Nm^{-2}; † Cm^{-2}; $^\hbar \times 10^{-9}$ Fm^{-1}.

3. Boundary Integral Equation

For a linear piezoelectric medium of volume Ω and boundary Γ, the following reciprocal relation can be established:

$$\int_\Gamma (\tau_i^{(2)} u_i^{(1)} - \tau_i^{(1)} u_i^{(2)} - q^{(2)}\phi^{(1)} + q^{(1)}\phi^{(2)})\, d\Gamma = \int_\Omega (F_i^{(1)} u_i^{(2)} - F_i^{(2)} u_i^{(1)} + \rho_e^{(2)}\phi^{(1)} - \rho_e^{(1)}\phi^{(2)})\, d\Omega \quad \textbf{(8)}$$

where the superscripts (1) and (2) denote two independent systems of field variables. In addition, τ_i and q are traction components in the i-direction and the surface charge respectively, in which,

$$\sigma_{ij} n_j = \tau_i ; \quad D_i n_i = q , \quad i, j = x, z \qquad \textbf{(9)}$$

and n_i denotes the outward unit normal vector in the i-direction.

Let the system (1) correspond to the actual problem and the system (2) to the fundamental solution. The reciprocal relation, Eq.(8), then becomes the following integral equation:

$$C(\mathrm{x}')U(\mathrm{x}') = \int_\Gamma G(\mathrm{x};\mathrm{x}')T(\mathrm{x})d\Gamma - \int_\Gamma H(\mathrm{x};\mathrm{x}')U(\mathrm{x})d\Gamma + \int_\Omega G(\mathrm{x};\mathrm{x}')F(\mathrm{x})d\Omega \qquad \textbf{(10)}$$

in which, for a smooth boundary Γ, the coefficient matrix C is given by

$$C(\mathrm{x}') = \begin{cases} I , & \mathrm{x}' \in \Omega \\ (1/2)I , & \mathrm{x}' \in \Gamma \\ 0, & \mathrm{x}' \notin \Omega \end{cases} \qquad \textbf{(11)}$$

where I and 0 denote an identity matrix and a zero matrix respectively. In addition,

$$U = \begin{Bmatrix} u_x \\ u_z \\ -\phi \end{Bmatrix}; \quad T = \begin{Bmatrix} \tau_x \\ \tau_z \\ -q \end{Bmatrix}; \quad F = \begin{Bmatrix} F_x \\ F_z \\ -\rho_e \end{Bmatrix} \qquad \textbf{(12)}$$

$$G = \begin{bmatrix} G_{xx} & G_{xz} & G_{xq} \\ G_{zx} & G_{zz} & G_{zq} \\ G_{qx} & G_{qz} & G_{qq} \end{bmatrix};$$

$$H = \begin{bmatrix} H_{xx} & H_{zx} & H_{qx} \\ H_{xz} & H_{zz} & H_{qz} \\ H_{xq} & H_{zq} & H_{qq} \end{bmatrix} \qquad \textbf{(13)}$$

In Eq.(13), G_{ij} (x; x´) and G_{iq} (x; x´) denote the displacement in the *i*-direction (*i* = *x, z*) at field point x due to a unit load in the *j*-direction (*j* = *x, z*) and a unit electric charge respectively applied at point x´ ; G_{qj} (x; x´) and G_{qq} (x; x´) denote the electric potential at field point x due to a unit load in the *j*-direction (*j* = *x, z*) and a unit electric charge respectively applied at point x´; H_{ij} (x; x´) and H_{iq} (x; x´) denote the traction in the *i* -direction (*i* = *x, z*) at field point x due to a unit load in the *j*-direction (*j* = *x, z*) and a unit electric charge respectively applied at point x´ ; H_{qj} (x; x´) and H_{qq} (x; x´) denote the electric charge at field point x due to a unit load in the *j*-direction (*j* = *x, z*) and a unit electric charge respectively applied at point x´.

In this paper, the fundamental solutions appear in the kernel matrices *G* and *H* corresponding to an infinite piezoelectric medium subjected to a unit concentrated line load in the *x*-and *z*-directions and a unit concentrated line electric charge given by Rajapakse [12].

The solutions for displacements and electric potential are expressed in terms of Fourier integral transforms as follows:

$$u_x = \frac{1}{2\pi}\int_{-\infty}^{+\infty}\left(i\xi\sum_{j=1}^{3}\beta_j M_j(\xi)\,e^{-\alpha_j|\xi|z}\right)e^{-i\xi x}\,d\xi \qquad \textbf{(14)}$$

$$u_z = \frac{1}{2\pi}\int_{-\infty}^{+\infty}\left(|\xi|\sum_{j=1}^{3}\eta_j M_j(\xi)\,e^{-\alpha_j|\xi|z}\right)e^{-i\xi x}\,d\xi \qquad \textbf{(15)}$$

$$\phi = \frac{1}{2\pi}\int_{-\infty}^{+\infty}\left(|\xi|\sum_{j=1}^{3}\delta_j M_j(\xi)\,e^{-\alpha_j|\xi|z}\right)e^{-i\xi x}\,d\xi \qquad \textbf{(16)}$$

where ξ denotes Fourier transform parameter; M_j are a set of arbitrary functions to be determined from the loading and boundary conditions; and α_j (j=1, 2, 3) are the roots of the following characteristic equation:

$$\alpha^6 + \omega_1\alpha^4 + \omega_2\alpha^2 + \omega_3 = 0 \qquad \textbf{(17)}$$

in which ω_1, ω_2 and ω_3 are real constants that depend on the electroelastic properties of a material. In addition,

$$\beta_i = (c_{13} + c_{44})(e_{33}\alpha_j^2 - e_{15})\alpha_j - (c_{33}\alpha_j^2 - c_{44})(e_{31} + e_{15})\alpha_j \qquad \textbf{(18)}$$

$$\eta_j = (c_{11} + c_{44}\alpha_j^2)(e_{33}\alpha_j^2 - e_{15}) - (c_{13} - c_{44})(e_{31} + e_{15})\alpha_j^2 \qquad \textbf{(19)}$$

$$\delta_j = -(c_{44}\,\alpha_j^2 - c_{11})(c_{44} - c_{33}\,\alpha_j^2) + (c_{13} + c_{44})^2\alpha_j^2 \qquad \textbf{(20)}$$

The solutions for stresses and electric displacements can then be obtained from Eqs.(14) to (16) by using Eqs.(1) to (5) and (7).

4. Numerical Implementation

In view of the complexity of the kernel matrices *G* and *H*, Eq.(10) is solved by applying numerical techniques. A numerical solution is obtained by discretizing the boundary Γ into a total of *NE* boundary elements. For the m^{th} boundary element (*m* = 1, 2,..., *NE*), the nodal values of the generalized displacements and traction can be expressed as

$$u = \langle u^{(1)} \quad u^{(2)} \quad \cdots \quad u^{(n)} \rangle^T ; \quad \tau = \langle \tau^{(1)} \quad \tau^{(2)} \quad \cdots \quad \tau^{(n)} \rangle^T \tag{21}$$

where

$$u^{(1)} = \langle u_x^{(i)} \quad u_z^{(i)} - \phi^{(i)} \rangle^T ; \quad \tau^{(i)} = \langle \tau_x^{(i)} \quad \tau_z^{(i)} \quad -q^{(i)} \rangle^T , \quad i = 1, 2, \cdots, n \tag{22}$$

and n is the total number of nodes for the m^{th} element.

According to the above discretization, Eq.(10) can be written in the absence of body force and electric charge as

$$C(\mathrm{x}')U(\mathrm{x}') = \sum_{m=1}^{NE} \left(\int_{\Delta\Gamma_m} G(\mathrm{x};\mathrm{x}')\, NJ d\Gamma\,(\eta) \right) \tau - \sum_{m=1}^{NE} \left(\int_{\Delta\Gamma_m} H(\mathrm{x};\mathrm{x}')\, NJ d\Gamma\,(\eta) \right) u \tag{23}$$

where J is Jacobian of transformation and η is the local coordinate. In addition, the shape function matrix $\boldsymbol{N}$ for the m^{th} element is given by

$$N = \left[N^{(1)} I \quad N^{(2)} I \quad \cdots \quad N^{(n)} I \right] \tag{24}$$

in which $N^{(i)}$ (i = 1, 2,···, n) denotes the shape function associated with the node i.

The numerical integration of Eq.(23) is performed by using the Gaussian integration technique. Special attention is required when the load point x´ coincides with the field point x and x the integration scheme presented by Watson [13] is implemented to calculate singular integrals. After performing the numerical integration over NE boundary elements, Eq.(23) can be expressed in the following form:

$$\mathcal{H}\mathcal{U} = \mathcal{G}\mathcal{T} \tag{25}$$

where the elements of the matrices $\mathcal{G}$ and $\mathcal{H}$ are obtained from the integrals of the first and the second terms respectively appearing in the right hand side of Eq.(23). Note that the C matrix in Eq.(23) is absorbed into the diagonal blocks of the matrix $\mathcal{H}$. In addition, $\mathcal{U}$ and $\mathcal{T}$ are column vectors whose elements are the nodal values of the generalized displacements and traction respectively.

Consider a piezoelectric domain consisting of two sub-regions with different material properties. Both sub-regions are connected along an interface Γ_I as shown in Fig. 2. The equation system for a sub-region k (k=1, 2) can be written as

$$\left[\mathcal{H}_B^k \quad \mathcal{H}_I^k \right] \begin{Bmatrix} \mathcal{U}_B^k \\ \mathcal{U}_I^k \end{Bmatrix} = \left[\mathcal{G}_B^k \quad \mathcal{G}_I^k \right] \begin{Bmatrix} \mathcal{T}_B^{\prime k} \\ \mathcal{T}_I^{\prime k} \end{Bmatrix} \tag{26}$$

where $\mathcal{U}_B^k$ and $\mathcal{T}_B^{\prime k}$ denote the nodal values of the generalized displacements and traction respectively on the external boundary Γ_B that belongs to the sub-region k ; $\mathcal{U}_I^k$ and $\mathcal{T}_I^{\prime k}$ denote the nodal values of the generalized displacements and traction respectively on the interface Γ_I that belongs to the sub-region k .

The compatibility and equilibrium conditions at the interface Γ_I require that

$$\mathcal{U}_I^1 = \mathcal{U}_I^2 ; \qquad \mathcal{T}_I^{\prime 1} = -\mathcal{T}_I^{\prime 2} \tag{27}$$

According to the above interface conditions, the final equation system then becomes

$$\begin{bmatrix} \mathcal{H}_B^1 & \mathcal{H}_I^1 & -\mathcal{G}_I^1 & 0 \\ 0 & \mathcal{H}_I^2 & \mathcal{G}_I^2 & \mathcal{H}_B^2 \end{bmatrix} \begin{Bmatrix} \mathcal{U}_B^1 \\ \mathcal{U}_I \\ \mathcal{T}_I \\ \mathcal{U}_B^2 \end{Bmatrix} = \begin{bmatrix} \mathcal{G}_B^1 & 0 \\ 0 & \mathcal{G}_B^2 \end{bmatrix} \begin{Bmatrix} \mathcal{T}_B^1 \\ \mathcal{T}_B^2 \end{Bmatrix} \tag{28}$$

The nodal solutions can be obtained by solving Eq.(28) with appropriate boundary conditions. It is noted that computations should be carried out with high order of precision to handle ill-conditioning of the matrix due to substantial difference in the order of magnitudes of the kernel functions in the boundary integral equation.

The solutions for displacements and electric potential within the domain Ω can be determined by substituting the nodal solutions from Eq.(28) into Eq.(23) with x´ ∈ Ω . The solutions for stresses and electric displacements within the domain can be computed by substituting the nodal solutions from Eq.(28) into the following equation with x´ ∈ Ω :

$$S(\mathrm{x}') = \sum_{m=1}^{NE} \left(\int_{\Delta\Gamma_m} G^S(\mathrm{x};\mathrm{x}')\, NJ d\Gamma(\eta) \right) \tau - \sum_{m=1}^{NE} \left(\int_{\Delta\Gamma_m} H^S(\mathrm{x};\mathrm{x}')\, NJ d\Gamma(\eta) \right) u \tag{29}$$

where S denotes the generalized stress vector defined as

$$S = \{\sigma_{xx} \quad \sigma_{zz} \quad \sigma_{zx} \quad D_x \quad D_z\}^T \tag{30}$$

and the two matrices $G^S$and H^S are obtained by differentiating the elements of matrices G and H given by Eq.(13) respectively with appropriate constitutive relations given by Eqs.(1) to (5).

5. Numerical Results and Discussion

The numerical solution scheme based on the boundary integral equation method described in the preceding sections has been implemented into a computer program to study piezoelectric bi-materials with an elliptical cavity under remote mechanical and electrical loading as shown in Fig. 1. The quadratic elements (three-node elements) are used and the following non-dimensional quantities are employed in the numerical results in this paper:

$$\sigma_{ij}^{*} = \sigma_{ij} / \sigma_0; \qquad \sigma_{ij}^{**} = \sigma_{ij} / D_0 \tag{31}$$

$$D_i^{*} = D_i / \sigma_0; \qquad D_i^{**} = D_i / D_0 \tag{32}$$

$$E_i^{*} = E_i / \sigma_0; \qquad E_i^{**} = E_i / D_0 \tag{33}$$

First, the convergence and stability of the present boundary element scheme are investigated with respect to number of elements *NE* and the dimension of the plane *W* (see Fig. 1). Non-dimensional stress (σ_{zz}^{*}) along the *x*-axis of an infinite PZT-4 plane with a circular hole (*b/a* = 1) under remote tension in the *z*-direction ($\sigma_{zz}^{\infty} = \sigma_0$) is shown in Fig. 3

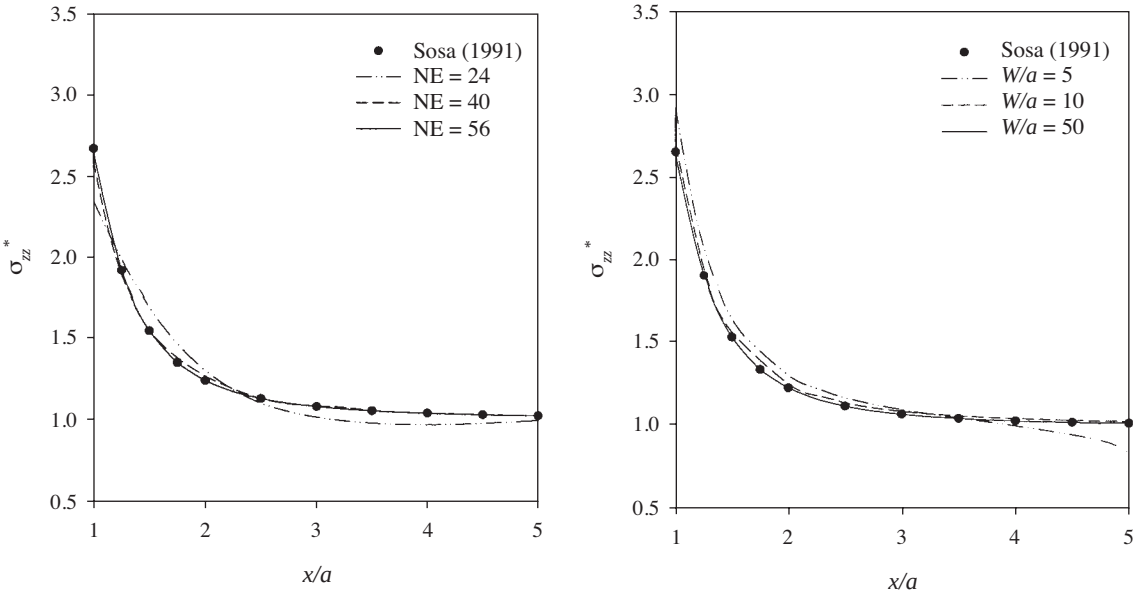

Fig. 3 Comparison of boundary element solutions.

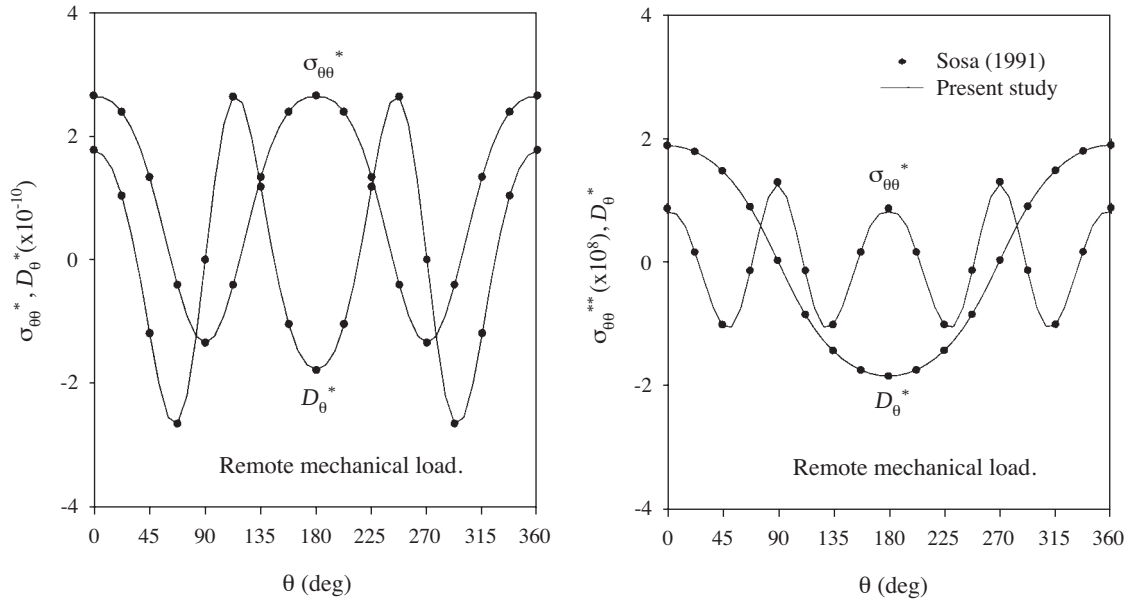

Fig. 4 Comparison with analytical solutions.

for different values of *NE* and *W/a*. The analytical solutions given by Sosa [1] are also presented for comparison. The boundary of the hole is traction-free and completely insulated, and the plane-strain condition is assumed. These conditions are employed for all numerical results presented in this paper. It has been found that numerically stable and converged solutions can be obtained when $NE \geq 56$ and the effect of the boundary on the solution becomes negligible if $W/a \geq 50$. Comparisons of

non-dimensional hoop stresses ($\sigma^{*}_{\theta\theta}$; $\sigma^{**}_{\theta\theta}$) and electric displacements (D^{*}_{θ} ; D^{**}_{θ}) around the circular hole with Sosa's solutions [1] are presented in Fig. 4 for remote tension ($\sigma^{\infty}_{zz} = \sigma_0$) and remote electric displacement ($D^{\infty}_{z} = D_0$) in the z-direction. It can be clearly seen from Fig. 4 that the present BEM solutions agree very closely with analytical solutions for both mechanical and electrical loads.

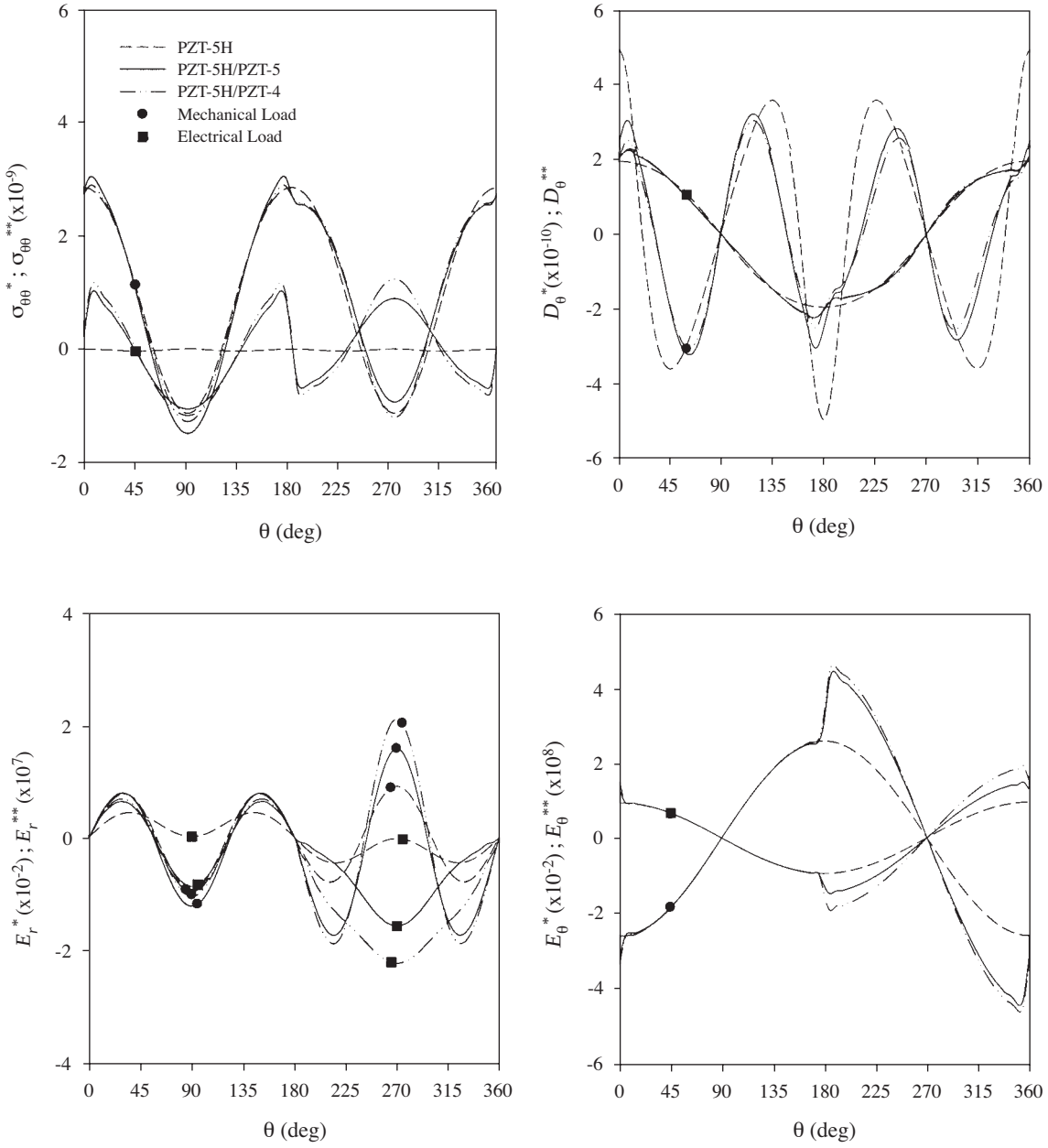

Fig. 5 Electroelastic fields around a circular cavity of different piezoelectric bi-materials.

Electroelastic response of piezoelectric bi-materials with an elliptical cavity at the interface subjected to remote tension ($\sigma_{zz}^{\infty} = \sigma_0$) and remote electric displacement in the z-direction ($D_z^{\infty} = D_0$) as shown in Fig. 1 is presented next. Fig. 5 presents electroelastic fields around a circular cavity (b/a=1) of different piezoelectric bi-materials, PZT-5H/PZT-5 and PZT-5H/PZT-4, and a piezoelectric material PZT-5H subjected to remote tension and electric displacement in the z-direction. The properties of all piezoelectric materials are given in Table 1. Numerical results in this figure indicate notable differences of electroelastic responses in piezoelectric materials and bi-materials, especially in the case of hoop stress under electrical loading, in which $\sigma_{\theta\theta}^{**}$ of the bi-materials (PZT-5H/PZT-5 and PZT-5H/PZT-4) is much higher than that of PZT-5H. On the other hand, higher electric displacement around the cavity under remote tension is observed in PZT-5H when compared to that of the bi-materials. Note that $\sigma_{\theta\theta}^{*}$ and D_{θ}^{**} for all three cases are not much different. In addition, the maximum electric field concentrations under both mechanical and electrical loads are found in the PZT-5H/PZT-4 bi-materials followed by PZT-5H/PZT-5 and PZT-5H respectively.

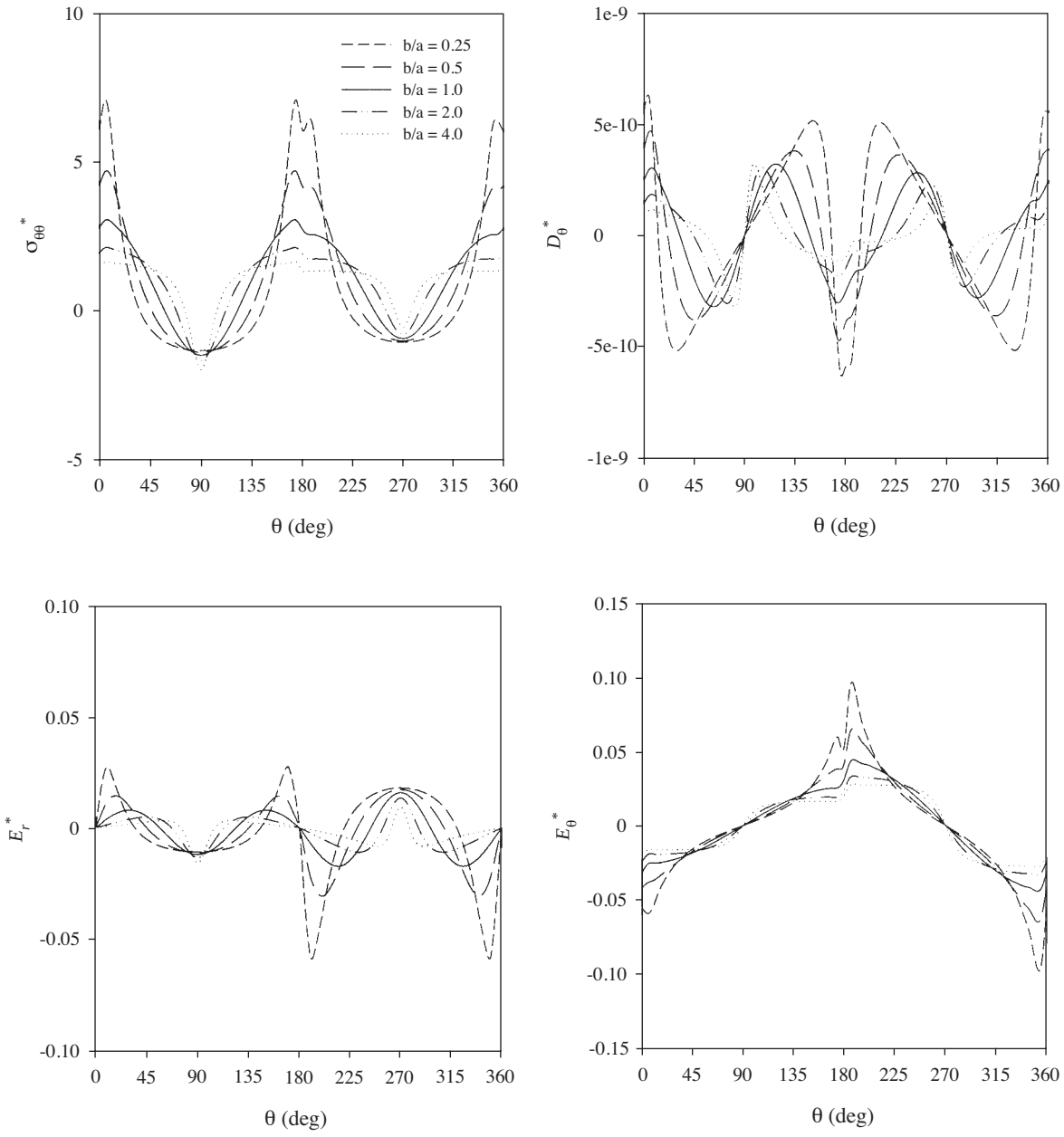

Fig. 6 Electroelastic fields around an elliptic cavity of PZT-5H/PZT-5 under remote tension.

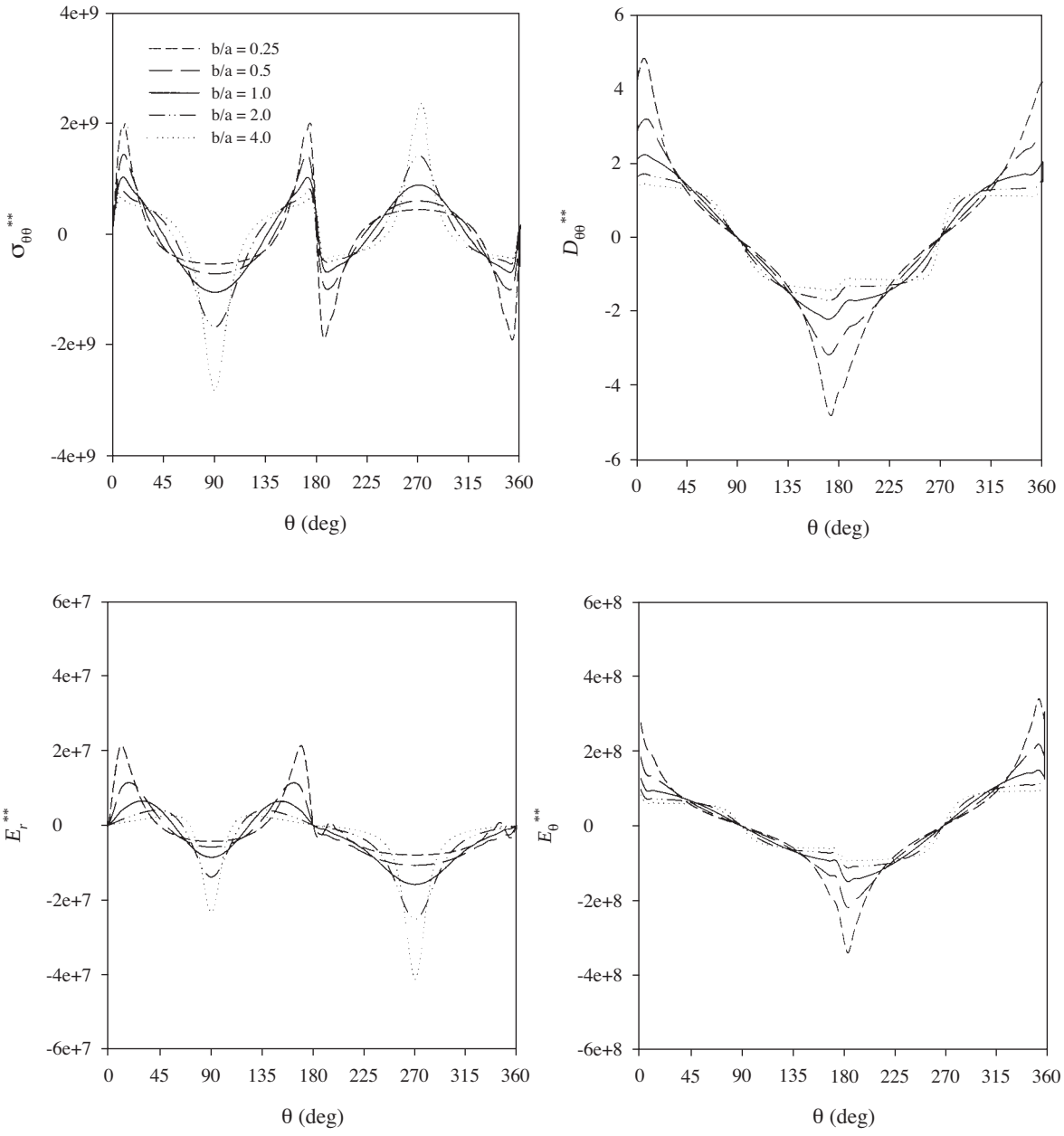

Fig. 7 Electroelastic fields around an elliptical cavity of PZT-5H/PZT-5 under remote electric displacement.

Fig. 6 presents electroelastic fields around the boundary of an elliptical cavity ($s^*_{\theta\theta}$, D^*_θ, E^*_r and E^*_θ) in piezoelectric bi-materials PZT-5H/PZT-5 under remote tension in the z-direction for different values of b/a (b/a = 0.25, 0.5, 1.0, 2.0 and 4.0). The solutions under remote electric displacement in the z-direction ($\sigma^{**}_{\theta\theta}$, D^{**}_θ, E^{**}_r and E^{**}_θ) are shown in Fig. 7. It can be clearly seen from Figs. 6 and 7 that electroelastic responses around the cavity boundary depend significantly on the ratio b/a. The solutions around the cavity boundary under remote tension shown in Fig. 6 decrease with increasing

the value of *b/a* and their maximum values are found in the vicinity of the interface of the two materials ($\theta = 0, \pi$). Numerical results presented in Fig. 7 for electrical loading indicate similar variation of circumferential electric displacement (D_q^{**}) and circumferential electric field (E_q^{**}) with q. The maximum values of D_q^{**} and E_q^{**} are found near the bi-material interface ($\theta = 0, \pi$) and they decrease with increasing the value of *b/a*. Hoop stress (σ_{qq}^{**}) and radial electric field (E_r^{**}) are zero at the bi-material interface ($\theta = 0, \pi$). In addition, their magnitudes along the boundary also decrease with increasing the geometric ratio *b/a* except in the vicinity of $q = \pi/2$ and $3\pi/2$.

6. Conclusions

Boundary element method is employed to investigate electroelastic responses of two-dimensional piezoelectric bi-materials by utilizing a sub-region model and a multi-region assembly. Convergence, numerical stability and accuracy of the present numerical solution scheme are established by comparing with existing analytical solution. Selected numerical results for electroelastic fields of piezoelectric bi-materials with an elliptical cavity under remote tension and remote electric displacement are presented. It has been found that significant differences between electroelastic responses of piezoelectric material and bi-materials are observed especially in the case of hoop stress under remote electric displacement. In addition, stresses, electric displacements and electric fields around the cavity depend significantly on the geometric ratio *b/a* and the type of loading. Stress and electric field concentrations decrease with increasing the value of *b/a* under mechanical loading and the maximum values are observed in the vicinity of the interface. For electrical loading, the maximum stress and electric field concentrations occur at different locations on the boundary depending on the geometry of the hole.

7. References

1. Sosa, H., 1991, "Plane Problems in Piezoelectric Media with Defects", *International Journal of Solids and Structures,* Vol. 28, No. 4, pp. 491-505.

2. Pak, Y.E., 1992. "Circular Inclusion Problem in Antiplane Piezoelectricity", *International Journal of Solids and Structures,* Vol. 29, No. 19, pp. 2403-2419.

3. Chung, M.Y. and Ting, T.C.T., 1996, "Piezoelectric Solid with an Elliptic Inclusion or Hole", *International Journal of Solids and Structures,* Vol. 33, No. 23, 3343-3361.

4. Sosa, H. and Khutoryansky, N., 1996, "New Developments Concerning Piezoelectric Materials with Defects", *International Journal of Solids and Structure,* Vol. 33, No. 23, pp. 3399-3414.

5. Lee, J.S., 1995, "Boundary Element Method for Electroelastic Interaction in Piezoceramics", *Engineering Analysis with Boundary Elements,* Vol. 15, No. 4, pp. 321-328.

6. Ding, H., Wang, G., and Chen, W., 1998, "A Boundary Integral Formulation and 2D Fundamental Solutions for Piezoelectric Media", *Computer Methods in Applied Mechanics and Engineering,* Vol. 158, No. 1-2, pp. 65-80.

7. Xu, X.-L. and Rajapakse, R.K.N.D., 1998, "Boundary Element Analysis of Piezoelectric Solids with Defects", *Composites Part B: Engineering,* Vol. 29, No. 5, pp. 655-669.

8. Liu, Y. and Fan, H., 2001, "On the Conventional Boundary Integral Equation Formulation for Piezoelectric Solids with Defects or of Thin Shapes", *Engineering Analysis with Boundary Elements,*

Vol. 25, pp. 77-91.

9. Pan, E., 1999, "A BEM Analysis of Fracture Mechanics in 2D Anisotropic Piezoelectric Solids", *Engineering Analysis with Boundary Elements,* Vol. 23, No. 2, pp. 67-76.

10. Davi, G. and Milazzo, A., 2001, "Multidomain Boundary Integral Formulation for Piezoelectric Materials Fracture Mechanics", *International Journal of Solids and Structures,* Vol. 38, No. 40-41, pp. 7065-7078.

11. Groh, U. and Kuna, M., 2005, "Efficient Boundary Element Analysis of Cracks in 2D Piezoelectric Structures", *International Journal of Solids and Structure,* Vol. 42, No. 8, pp. 2399-2416.

12. Rajapakse, R.K.N.D., 1997, "Plane Strain/Stress Solutions for Piezoelectric Solid", *Composites Part B: Engineering,* Vol. 28, No. 4, pp. 385-396.

13. Watson, J.O., 1979, *Advanced Implementation of Boundary Element Method in Two and Three-dimensional Elastostatics,* In: Banerjee, P.K. and Butterfield, R. (Eds.), Developments in Boundary Element Methods, Elsevier, London, UK, Vol.1, Chapter 3.